Polyvinyl Alcohol/Hydroxyethylcellulose Containing Ethosomes as a Scaffold for Transdermal Drug Delivery Applications

Gomaa El Fawal, Huoyan Hong, Xinran Song, Jinglei Wu, Meiqi Sun, Lin Zhang, Chuanglong He, Xiumei Mo & Hongsheng Wang

Applied Biochemistry and Biotechnology

ISSN 0273-2289

Appl Biochem Biotechnol
DOI 10.1007/s12010-020-03282-1

Springer

Applied Biochemistry and Biotechnology
https://doi.org/10.1007/s12010-020-03282-1

Polyvinyl Alcohol/Hydroxyethylcellulose Containing Ethosomes as a Scaffold for Transdermal Drug Delivery Applications

Gomaa El Fawal[1,2] · Huoyan Hong[1] · Xinran Song[1] · Jinglei Wu[1] · Meiqi Sun[1] · Lin Zhang[3] · Chuanglong He[1] · Xiumei Mo[1] · Hongsheng Wang[1]

Received: 14 November 2019 / Accepted: 13 February 2020/Published online: 21 March 2020

Abstract
This study aims to develop scaffold for transdermal drug delivery method (TDDM) using electrospinning technique from polyvinyl alcohol (PVA) and hydroxyethylcellulose (HEC). The fluorescein isothiocyanate (FITC) loaded on ethosomes (FITC@Eth) was used as a drug model. The prepared PVA/HEC/FITC@Eth scaffold was characterized via scanning electron microscope (SEM) that show morphology change by adding FITC@Eth. Also, Fourier transform infrared spectroscopy (FTIR), mechanical properties, X-ray diffraction (XRD), thermal gravimetric (TGA) analysis show that the addition of FITC@Eth to PVA/HEC does not change the scaffold properties. Franz diffusion cells were used for in vitro skin permeation experiments using rat dorsal skins. The FITC@Eth penetration was better than that of free FITC due to the presence of ethosome which enhance the potential skin targeting. In conclusion, the prepared PVA/HEC/FITC@Eth scaffold can serve as a promising transdermal scaffold for sustained FITC release.

Keywords Transdermal drug delivery · Polyvinyl alcohol (PVA) · Hydroxyethylcellulose · Ethosomes

✉ Lin Zhang
zhanglinfudan@zju.edu.cn

✉ Hongsheng Wang
whs@dhu.edu.cn

[1] Key Laboratory of Science & Technology of Eco-Textile, Ministry of Education, College of Chemistry, Chemical Engineering and Biotechnology, Donghua University, Shanghai 201620, China

[2] Polymer Materials Research Department, Advanced Technology and New Materials Research Institute, City of Scientific Research and Technological Applications (SRTA-City), New Borg El-Arab City, Alexandria 21934, Egypt

[3] Department of Pharmacy, Shaoxing People's Hospital, Shaoxing Hospital of Zhejiang University, Shaoxing 31200, China

Introduction

Electrospinning is a technique used to generate micro/nanofibrous mats from polymeric solutions or melts (natural and synthetic). The flexibility of this technique facilitates the electrospun mats production for different applications fields [1, 2]. Transdermal drug delivery method (TDDM) – particularly scaffold carrier – have attracted more attention because it avoids the first-pass metabolism for the drugs and could give constant blood levels for a long time [3]. TDDM is a method for drug delivery via the skin to reach systemic or local effect. It became one of the third-generation of pharmaceutical preparations after injection and oral medication [4]. This refers to the way of using drugs, which is non-invasive, easy to use, and enhance patient compliance [5]. TDDM offers steady plasma levels and simple detection of the drug and overdose lower chances [6]. Besides, it avoids the gastrointestinal environment interaction on drug efficacy like enzymatic action, pH, and the interfering between food and drug [7]. Drugs application in TDDM is limited because of the drug resistance that comes from stratum corneum (SC) during the percutaneous permeation [8]. SC is the outer layer of the epidermis – it is the most important protective layer of the skin and contact with the external environment [9]. SC layer cells are similar to the semipermeable membrane, this causes the delivery of hydrophilic macromolecules across the skin is hard and the target transdermal rate is difficult to reach [9, 10]. Therefore, many methods have been used to increase the efficiency of transdermal applications like electroporation, iontophoresis, chemical enhancers, magnetophoresis, and sonophoretic [11].

Ethosomes (Eth) has been used as a carrier to improve the amount of drug permeation through the skin in the TDDM [7]. Eth are composed of alcohol, phospholipids, and water [10]. In addition, it has a stable structure, small particle, and high encapsulation efficiency [12]. Also, Eth can significantly enhance drug accumulation in the skin by increasing drug penetration into the skin [13]. Many materials used during formulation of ethosomes like rhodamine [12], cholesterol (vesicle membrane stabilization) [14], pluronic F-127 [15], poloxamer 407 [16], and carbopol [17].

Recently, polyvinyl alcohol (PVA) was used as an effective transdermal delivery carrier [18]. PVA is a water-soluble, nontoxic, biocompatible, and biodegradable synthetic polymer with excellent electrospinnability and has been widely applied in the biomedical applications [18]. It provides flexibility and mechanical stability to the traditional scaffolds prepared from natural polymers [4]. PVA is non-adhesive polymer toward the live cells and so it blended with polysaccharides to enhance its adhesion [19]. Polysaccharides are biodegradable carbohydrates come from natural sources like chitosan, gelatin, agarose, alginate, and starch [20]. It has been used in many applications like biomedical, food packaging, and water treatment [20–24]. Hydroxyethylcellulose (HEC) – a cellulose ethers derivative – has usually used in many biotechnological and industrial applications because of its chemical compositions and water solution properties [25–27].

This study aims to prepare scaffold from PVA and HEC via electrospinning technique to promote drugs transdermal delivery effect. Fluorescein isothiocyanate loaded on ethosome (FITC@Eth) was used as the model drug. Thermal gravimetric analysis (TGA) was used to examine the thermal change of PVA/ HEC and PVA/HEC/FITC@Eth scaffold. Also, scanning electron microscopy (SEM), Fourier-transform infrared spectroscopy (FTIR), X-ray diffraction (XRD), and mechanical properties of the scaffolds were examined. The transdermal delivery test was applied in vitro to evaluate the permeation and the cumulative release of FITC from PVA/HEC/FITC@Eth through the skin.

Materials and Methods

Materials

Poly (vinyl alcohol) (MW ~146,000–186,000), hydroxyethylcellulose (average MW ~90,000), and fluorescein isothiocyanate (FITC) were purchased from Sigma-Aldrich (Shanghai, China). Glutaraldehyde aqueous solution (25%), cholesterol and lecithin were purchased from Merck (Germany). All other used chemicals were laboratory grade.

Preparations of PVA/HEC Solutions

PVA solution (12 wt.%) was prepared in distilled water with stirring for 2 h at 80 °C. The HEC powder (6 wt.%) was dissolved in distilled water with stirring for 1 h at 60 °C. PVA/HEC blend solutions were prepared by mixing them at 50:50, 70:30, and 90:10 ratio with continuously stirring for 3 h. Table 1 illustrate the electrospinning parameters and blended solutions ratio. Brokefield LV viscometer was used to measure the viscosity (at room temperature with the shear rate of 15 s^{-1} and CyberScan Bench pH/mV Meter was used to measure the electrical conductivity. For electrospinning, 10 mL of each blend solution was pumped through a 20-gauge needle to obtain the nanofiber scaffold. Then, the membranes were incubated in a desiccator containing glutaraldehyde vapor – at room temperature – for 3 h. After that, the membranes were kept in a vacuum oven (at room temperature) to dry overnight before characterization.

Preparation of Ethosomes

Ethosome was prepared according to phase reversion method [28]. Briefly, 10 mg cholesterol and 100 mg lecithin were dissolved in 5 mL ethanol, then this solution was evaporated by rotary evaporator to get a dry film. Finally, 10 mL of H_2O/ethanol (8:2 in volume) was used to dissolve the dry film to get the ethosome. FITC (5, 10, and 15 μg/mL) was added to the ethosome solution and sonicated for 30 s. to get uniformly dispersed FITC@Eth. Then, the FITC@Eth solution was stirred for 2 h (at room temperature) to dissolve completely FITC.

Electrospray Method

PVA (0.5 g) dissolved in 6 mL ethanol (60%) and then added 4 mL of FITC@Eth (prepared in the previous step) to it with stirring for 1 h to get a clear solution. The electrospray conditions are 10 Kv, 10 cm, and 1 mL/h.

Table 1 Polymer blends ratio, properties, and electrospinning parameters

Polymer blends	Voltage (kV)	Flow rate (mL/h)	Tip-to collector distance (cm)	Viscosity (cP)	Conductivity (μS/cm)
PVA	13	0.5	17	4295	2115
HEC	–	–	–	47	213
PVA/ HEC (90:10)	15	0.4	12	3121	1645
PVA/ HEC (70:30)	17	0.5	17	2345	1432
PVA/ HEC (50:50)	18	0.5	17	514	768

In Vitro Transdermal Performance of the Modified Ethosomes

Skin Preparation

The surface hair of dead rat was removed by a shaver and the skin was removed. Isopropanol alcohol was used to wipe the dermis side to remove the remaining adhering subcutaneous. Then, the obtained skin was washed many times with PBS (pH = 7.4) and stored at −20 °C until further use.

Skin Permeation Study

Franz diffusion method was used for the transdermal test for FITC loaded on the ethosomes (FITC@Eth) as a drug model. The receptor compartments were filled with PBS buffer (pH = 7.4) as a receiving liquid. Moreover, circulating water bath was used to keep PBS under stirring at 37 °C. The suitable size of the rat skin specimen was placed between the receptor and donor of the Franz diffusion cell system – the stratum corneum facing the scaffold containing FITC@Eth [29]. Free FITC (10%) in H_2O/ethanol (8:2 in volume) was used as a control group. At specific interval times, 2 mL of the receptor solution was taken and then replaced by an equal volume of fresh buffer. The collected samples were evaluated for drug permeation by determine drug cumulative release using a UV–vis spectrophotometer (485 nm).

The cumulative release was calculated using the following equation:

$$Q = \frac{CVn + \sum_{i=1}^{n-1} CiVi}{Q'} X\ 100$$

Where Q is the cumulative release amount, C and V are the drug concentration and volume of the receiving liquid in the diffusion cell, Q' is the amount contained in Eth, C_i is the drug concentration at the time of the sampling, and V_i is the volume at the time of sampling.

Physico-Chemical characterization

Morphology of Electrospun Scaffold

Scanning electron microscope (SEM, Hitachi TM-100, Japan) was used to observe the electrospun scaffold morphology – under 15 kV accelerating voltage. The samples were coated with gold before observation under SEM.

Fourier Transform Infrared Spectroscopy (FT-IR)

Fourier transform infrared spectroscopy (FTIR-Thermo Nicolet 6700) was used to examine chemical interaction between PVA and HEC. The absorbance range of 400–4000 cm^{-1} with a resolution of 2 cm^{-1} and 16 scans per run was used.

Thermal Gravimetric Analysis (TGA)

The thermal stability of electrospun scaffold was determined by Shimadzu thermal analyzer 50 (Japan). The nitrogen atmosphere was used (20 mL/min flow) in the range 40–600 °C with heating rate 10 °C/min. The graph was plotted with weight (mg) vs. temperatures.

X-Ray Diffraction (XRD) Analysis

Shimadzu X-ray diffraction (7000, USA, Cu-Kα radiation) was used to examine the crystallinity of electrospun scaffold at 1.5406 Å wavelength. The data were collected in the range of $10 \leq 2\theta \leq 60°$ – in the form of 2θ versus intensity (a.u) chart.

Mechanical Properties

Universal Materials Testing Machine (H5K-S, Hounsfield, UK) was used to examine the mechanical properties (tensile strength (TS) and elongation at break (E%)) – at room temperature. The cross-head speed was 5 mm/min to test all specimens (10 mm × 30 mm, $n = 3$). The electronic digital micrometer (Mitutoyo, Japan) was used to measure specimen thickness. "E" expresses the percentage change of initial gauge length for the specimen (30 cm) at the point of its failure. "TS" was considered by dividing force (maximum load) by the initial cross-sectional area of a specimen.

Results and Discussion

PVA polymer is an easily electrospun polymer while HEC cannot form nanofiber alone and so PVA was used to increases the spinnability of HEC. After many trials, PVA (12%), HEC (6%), and three ratios of PVA: HEC were used for the electrospinning (Table 1). The electrospinning condition changed depending on the ratio between PVA and HEC. The different ratio has different solution properties (viscosity and conductivity) (Table 1). The polymer solution viscosity has a strong effect on the electrospinning process [2, 30]. It has been found that there are beads or beaded fibers formation with very low viscosity as the surface tension is the dominant factor and with very high viscosity there is difficulty in the ejection of jets from polymer [31]. Those results agree with the work of Chahal et al. for PVA and HEC [32]. They found that the increase in the HEC ratio leads to a decrease in the viscosity and conductivity of the PVA/HEC solution. HEC solution alone and the high HEC contained solution form beads instead of nanofiber (compared to PVA alone) because the HEC solution properties (viscosity and conductivity) are lower than PVA (Table 1, Fig. 1). When we added FITC@Eth to PVA/HEC solution, the electrospinning condition was changed depending on the new solution composition, and it became difficult to get the nanofibers as the viscosity and conductivity became lower than the optimized PVA/HEC solution. The viscosity and conductivity become 1750 cP and 1250 μS/cm when we use FITC (10 mg/mL). In this case, we used the electrospray method to added FITC@Eth on the surface of PVA/HEC scaffold. The electrospray method has many advantages like low-cost, low-energy, and single-step material processing technology. Also, it is easy to control coating thickness and deposition rate through flow rate and voltage at atmospheric conditions [33].

Morphology Nanofibrous Scaffolds

The SEM micrograph (Fig. 1) shows a non-woven, bead-free, porous, and uniform morphology for PVA/HEC blends (100:0, 90:10). The average fiber diameter for the PVA/HEC (90:10) was 479.14 ± 37 nm (using *ImageJ*®), similar results were reported for PVA/HEC nanofibers for bone tissue engineering [32]. Further addition of HEC up to 50% led to the formation of fibers and beads. This due to the change in the viscosity and conductivity of the solution (Table 1). The electrospray method used to add the active drug on the mate's surface (Fig. 2). The nanofiber morphology was changed by adding the FITC@Eth on the surface. The nanofiber diameter increases from 479.14 ± 37 to 515 ± 22 nm by using 15 μg/mL FITC@Eth (Fig. 2a). The increases in the nanofiber diameter come from the addition of PVA/FITC@Eth on the surface of PVA/HEC. Because the ethosome has a spherical shape, we find spherical particles appear on the mat's surface with irregular distributions [34]. The presence of some aggregation comes from different extents of electrostatic stretch during electrospray. Those results agree with the work of Kostakova et al. when they incorporated spherical hydroxylated fullerene on the PVA surface by electrospraying method [35].

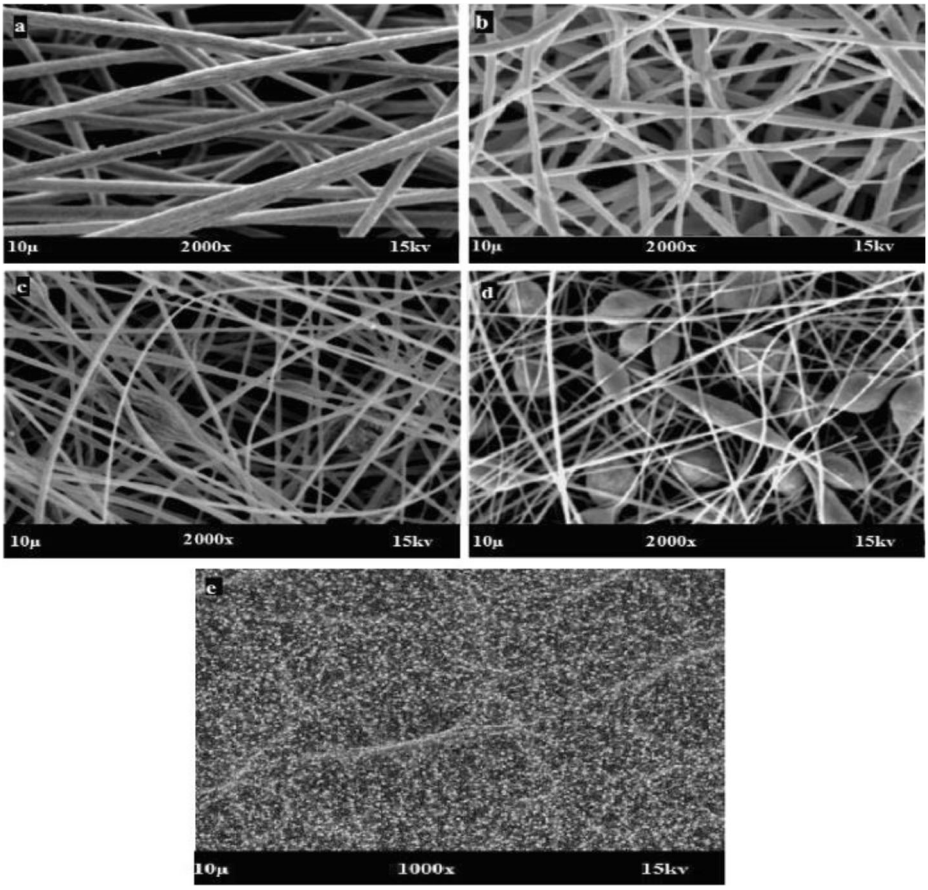

Fig. 1 SEM images of electrospun nanofibers for PVA/HEC blends (a) 100:00, (b) 90:10, (c) 70:30, (d) 50:50, and (e) 00:100

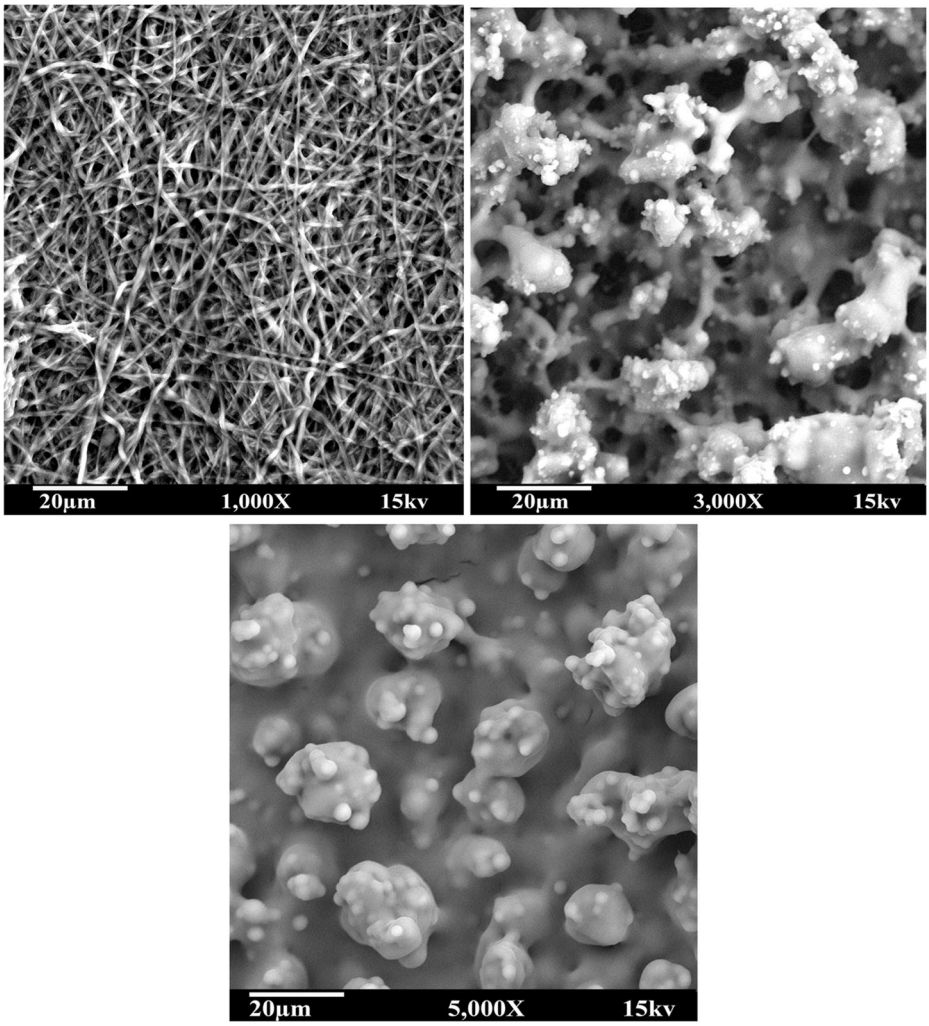

Fig. 2 SEM images of electrospun nanofibers for PVA/HEC/FITC@Eth (PVA: HEC, 90:10; FITC@Eth, 15 µg/mL)

FTIR Spectroscopy Analysis

Figure 3 shows the FTIR spectra of the PVA, HEC, PVA/HEC, and PVA/HEC/FITC@Eth. FTIR spectra for PVA illustrates band at 3303 cm^{-1} refer to the O-H group stretching while the C-H from alkyl groups appear at 2944 cm^{-1}. C=O and C-O have peaks at 1655 cm^{-1} and 1709 cm^{-1} (from acetate group remaining in PVA), while CH_2 has bending vibrations peaks at 1429 cm^{-1}. Those results agree with earlier work of Zulkifli et al., Andrade et al., and Coates for PVA [36–38]. HEC spectra show a peak at 3376 cm^{-1} and 2929 cm^{-1} refer to O-H and C-H aliphatic stretching vibrations, respectively. There are a specific band at 1463 cm^{-1} and 1354 cm^{-1} that refer to amorphous region characteristic and heterogeneous distribution of the substituted groups in the polymer chains. Peaks at 888 cm^{-1} and 1354 cm^{-1} represent C-O-C and C-O-H vibrations. All these peaks are in good agreement with the literature for HEC [39–41]. PVA/HEC blend spectra exhibited the combination of main peaks of PVA and HEC.

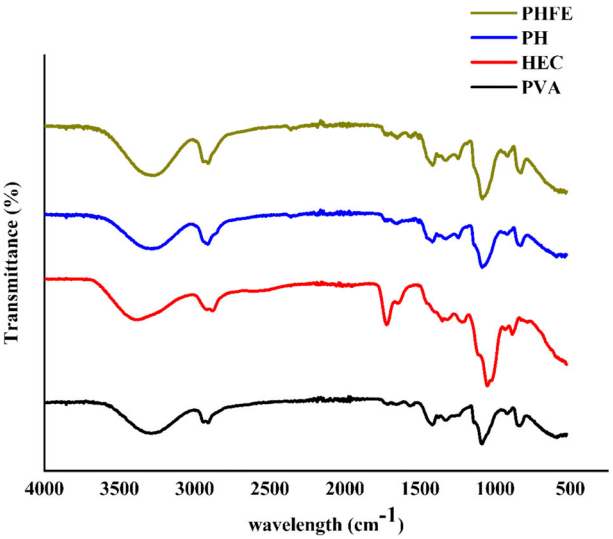

Fig. 3 FTIR spectra of the PVA, HEC, PVA/HEC (PH), and PVA/HEC/FITC@Eth (PHFE) (PVA/HEC, 90:10; FITC@Eth, 15 μg/mL)

The intensity of OH stretching has a slight effect due to the interacting between –OH groups on the PVA and HEC. Those results agree with earlier work of Qua et al. and Chahal et al., for PVA/microcrystalline cellulose and PVA/HEC [32, 42]. Free FITC has bands at 1204 cm^{-1}, 1503 cm^{-1}, and 1635 cm^{-1}, which related to the vibration of C=S, C=C, and C=O bonds, respectively [42–44]. PVA/HEC/FITC@Eth spectra show that the FITC bands overlap with that of PVA/HEC and there is no change in PVA/HEC spectra.

Mechanical Properties

The scaffold should have good mechanical properties to be used in a transdermal application to facilitate the active material permeation through stratum corneum. PVA blank scaffold shows tensile strength of 2.5 ± 0.3 MPa and elongation ~200% (Fig. 4). Those results agree with the

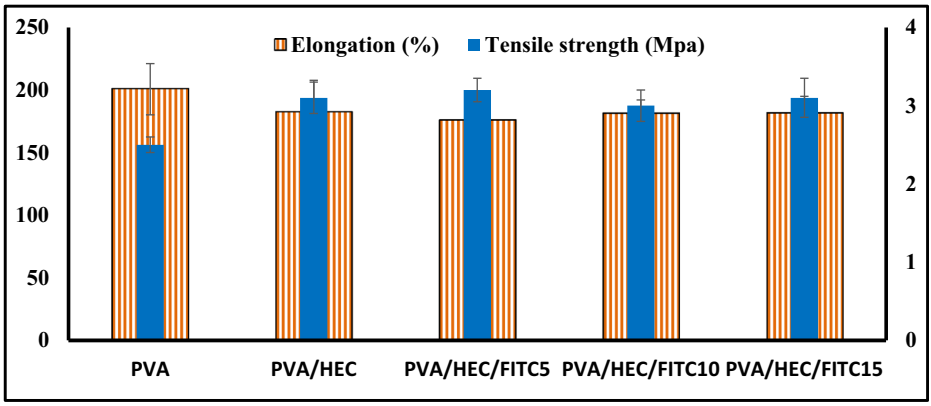

Fig. 4 Mechanical properties of PVA/HEC (PH) and PVA/HEC/FITC@Eth (PHFE) nanofibers (tensile strength and elongation (%)) (PVA/HEC, 90:10; FITC@Eth, 5, 10, and 15 μg/mL)

work of Chahal et al. when used PVA and HEC to prepare nanofibrous composite for bone tissue engineering [32]. They get tensile strength and elongation 2.6 ± 0.75 MPa and ~110%, respectively, for PVA. Adding HEC to PVA improve tensile strength to become 2.9 ± 0.5 MPa and decrease elongation. This behavior refers to the HEC molecules distribute between PVA molecules and promote the intrinsic properties of PVA. Those results agree with earlier work used PVA and HEC and it was found improvement in the mechanical properties (tensile strength and elongation) of the blend [31, 45, 46]. But our results do not agree with work of Chahal et al., as they stated that the elongation is increased by increasing the HEC ratio, but in our results, the elongation decrease when HEC ratio increase due to the interaction between PVA and HEC molecules that enhance tensile and decrease elongation. The mechanical properties for PVA/HEC/FITC@Eth scaffold are nearly unchanged by adding FITC@Eth. This refers to the addition of FITC@Eth using electrospray on the surface of the scaffold, not inside the scaffold matrix.

Thermogravimetric Analysis

Figure 5 shows TGA thermograms as a function of temperature for PVA, HEC, PVA/HEC, and PVA/HEC/FITC@Eth scaffolds. The thermograms figure shows three main stages for PVA and PVA/HEC/FITC@Eth scaffolds and two main stages for HEC. These steps and percentage mass loss were clear during heating in the mass loss diagram (TGA %) and Table 2. In the first stage – 40 °C to 158.4 °C – PVA and HEC polymers show 3.6% and 4.7% weight loss, respectively. The second stage − 135.6 to 478.6 °C – for PVA and HEC shows significant weight loss about 75.9% and 72.4%, respectively. The third stage – 375.9 °C to 577 °C – for PVA displays weight loss of 11.4%. Similar results were reported by Chahal et al. and Zulkifli et al., when used PVA and HEC to prepare composite for tissue engineering [32, 36]. PVA/HEC and PVA/HEC/FITC@Eth thermogram show three degradation steps that refer to the presence of more than one degradation stage [47]. This

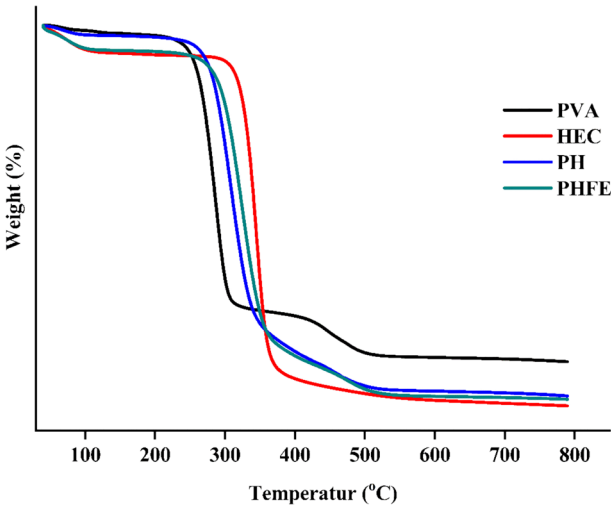

Fig. 5 TGA analysis for pure PVA, HEC, PVA/HEC (PH), and PVA/HEC/FITC@Eth (PHFE) scaffolds (PVA/HEC, 90:10; FITC@Eth, 15 μg/mL)

Table 2 TGA and DrTGA data for PVA, HEC, PVA/HEC (PVH), and PVA/HEC/FITC@Eth (PVHE) scaffolds

Sample	Region of decomposition	Temperature (°C)			Weight loss (%)	
		T_{start}	T_{end}	T_{peak}	Partial	Total
PVA	1	40	135.6	56.5	3.6	90.9
	2	135.6	375.9	285.9	75.9	
	3	375.9	577	421.6	11.4	
HEC	1	40	158.4	59.3	4.73	77.16
	2	148.5	478.6	330.3	72.43	
PVH	1	40	165.6	72.3	4.2	98.3
	2	165.6	425.9	279.3	88.1	
	3	425.9	574	447.9	6	
PVHE	1	40	175.4	60.5	7.3	97.9
	2	175.4	430.6	276.3	85.7	
	3	430.6	580.2	447.5	4.9	

**PVA/HEC, 90:10; FITC@Eth, 15 μg/ml*

suggests that adding PVA improve HEC thermal stability as the PVA is more thermal stable than HEC. The first stage – 40 °C to 175.4 °C – for PVA/HEC and PVA/HEC/FITC@Eth shows a weight loss percentage of 4.2% and 7.3%, respectively. The second stage – 165.6 °C to 430.6 °C – has a high weight loss of 85.7% and 88.1%. The third stage – 430.6 °C to 580.2 °C – for PVA/HEC/FITC@Eth shows weight loss percentage of 4.9%. For all thermograms, the results show that the first stage comes from moisture evaporation due to the thermal process [46] . Moreover, the second stage contains polymers degradation due to the bond broken in the polymeric chain (carbon-carbon bonds) that comes from PVA side-chain degradation and CO_2 loss from HEC [46]. Finally, the third stage refers to PVA by-products generated during the decomposition of PVA main chain [24, 48].

X-Ray Diffraction Analysis

Figure 6 shows the X-ray diffraction pattern of PVA, HEC, PVA/HEC, and PVA/HEC/FITC@Eth scaffold. The X-ray diffraction pattern of PVA has three peaks at $2\theta = 19.58°$, 22.84°, and 40.86° with corresponding d-spacing 4.53 A°, 3.89 A°, and 2.207 A°, respectively. These peaks appear because of intermolecular interference between PVA chains and this agrees with Ali work when using PVA and silver nanoparticles for antibacterial application [49]. The plane reflection (101) and (200) show scattering diffuse as a distinctive amorphous and crystalline phase of semi-crystalline PVA polymer [49, 50] . HEC displays a peak at 21.11° with the corresponding d-spacing of 4.203 A°. Due to the optically clear nature of HEC, it displays the liquid-like x-ray pattern as it is glassy amorphous polymer. Those results agree with earlier results of Attia et al. when studied structural and thermal characterization of PVA and HEC films [50]. Also, the results agree with the work of Chen et al. when studied the degradation of HEC [40]. The PVA/HEC scaffold display X-ray pattern peaks of PVA and HEC. It displays a diffraction peak at 22.54° related to HEC and peaks at 18.762° and 19.5° related to PVA that confirm the interaction between the polymers. Similar results were reported for PVA and hydroxypropyl cellulose (HPC) [47]. The PVA/HEC/FITC@Eth scaffold show similar results like PVA/HEC that confirm the addition of FITC@Eth to PVA/HEC do not affect the diffraction pattern of the scaffold.

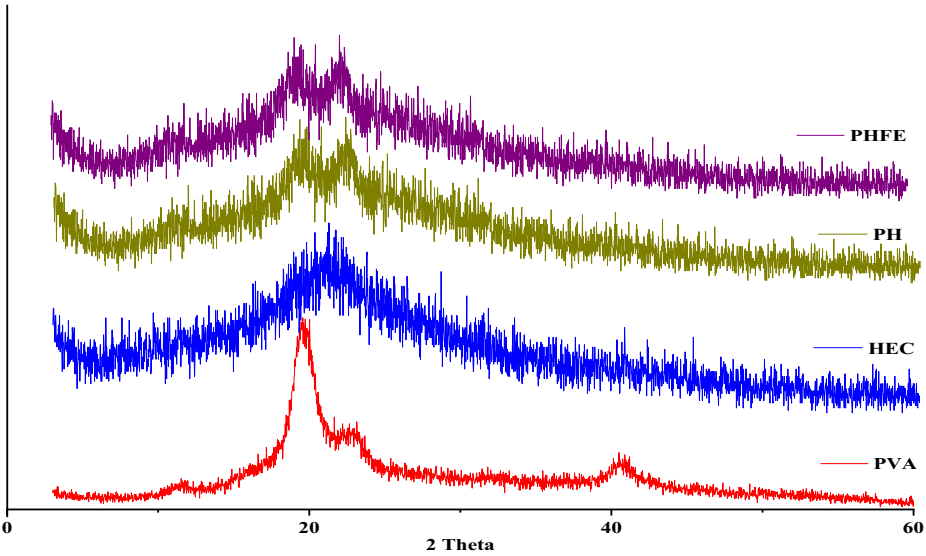

Fig. 6 XRD patterns of PVA, HEC, PVA/HEC (PH), and PVA/HEC/FITC@Eth (PHFE) (PVA/HEC, 90:10; FITC@Eth, 15 μg/mL).

Evaluation of Skin Permeability of the Modified Ethosomes In Vitro

The drug release parameter is a vital factor for transdermal application in the biomedical drug delivery studies. The release profile FITC from PVA/HEC/FITC@Eth scaffold are calculated by the FITC-eluting from the scaffold (Fig. 7). The release profile shows burst release through the first 12 h of release time, and the cumulative release rates during 48 h of FITC were 33.2%, 39.5%, and 43.5% – this release trend increases according to FITC content increases. The

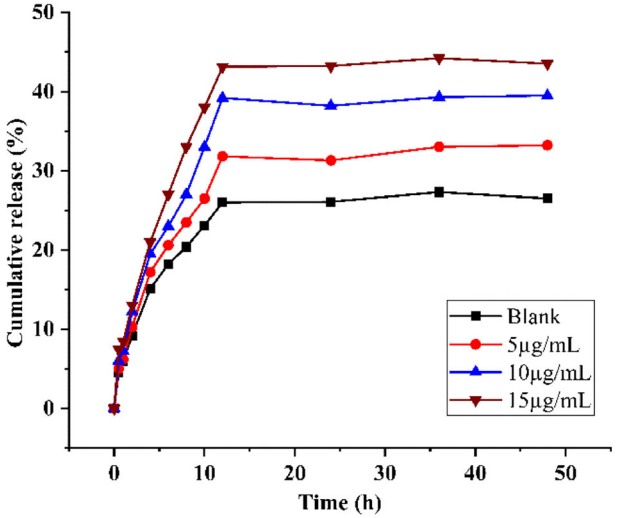

Fig. 7 Cumulative release (%) of FITC from PVA/HEC/FITC@Eth (PHFE) through rat skin

release of all FITC@Eth samples higher than that of the control group with free FITC (26.5%). Those results refer to the ethanol contained in ethosomes that increase effectively the mobility and deformability of ethosome through the rat skin [13, 51]. FITC transported into the skin cells by direct diffusion through cytomembrane. The ethosomes cause membrane fusion during the process of endocytosis – due to its lipids composition– which enhances the cellular uptake of the drugs loaded in ethosomes [9, 52].

Conclusion

PVA/HEC/FITC/@Eth scaffold was successfully fabricated using the electrospinning technique and optimized. FTIR analysis indicated the interaction between PVA and HEC. Thermal gravimetric analysis (TGA) and X-ray diffraction (X-rd) confirmed the presence of PVA and HEC in the scaffold. The skin permeation study was examined using FITC as a drug model. The cumulative release trend for FITC increased remarkably by using ethosome from 26.5% (free FITC) to 43.5% (PVA/HEC/FITC@Eth). In conclusion, the prepared PVA/HEC scaffold could be a promising material for the transdermal application.

Funding Information This research was supported by Shanghai Science and Technology Committee Project (18490740400), the Fundamental Research Funds for the Central Universities (2232019D3-20), the Project of Shaoxing Medical Key Discipline Construction Plan (NO. 2019SZD06), Opening project of Zhejiang provincial preponderant and characteristic subject of key university (traditional Chinese pharmacology), Zhejiang Chinese Medical University (ZYAOX2018035) and Project of Health and Family Planning Commission of Zhejiang province (2018KY831).

Compliance with Ethical Standards

Conflict of Interest The authors declare that they have no conflict of interest.

References

1. Asmatulu, R., & Khan, W. S. (2019). In R. Asmatulu & W. S. Khan (Eds.), *In Synthesis and applications of electrospun nanofibers* (pp. 17–39). Elsevier.
2. El Fawa, G.F. (2019). Polymer nanofibers electrospinning: A review. Egyptian Journal of Chemistry, in press; https://doi.org/10.21608/ejchem.2019.14837.1898.
3. Mendes, A. C., Gorzelanny, C., Halter, N., Schneider, S. W., & Chronakis, I. S. (2016). Hybrid electrospun chitosan-phospholipids nanofibers for transdermal drug delivery. *International Journal of Pharmaceutics, 510*, 48–56.
4. Kataria, K., Gupta, A., Rath, G., Mathur, R. B., & Dhakate, S. R. (2014). In vivo wound healing performance of drug loaded electrospun composite nanofibers transdermal patch. *International Journal of Pharmaceutics, 469*, 102–110.
5. Barry, B. W. (1987). Mode of action of penetration enhancers in human skin. *Journal of Controlled Release, 6*, 85–97.
6. Marwah, H., Garg, T., Goyal, A. K., & Rath, G. (2016). Permeation enhancer strategies in transdermal drug delivery. *Drug Delivery, 23*, 564–578.
7. Verma, P., & Pathak, K. (2010). Therapeutic and cosmeceutical potential of ethosomes: An overview. *Journal of Advanced Pharmaceutical Technology and Research, 1*, 274–282.
8. Cevc, G., & Blume, G. (1992). Lipid vesicles penetrate into intact skin owing to the transdermal osmotic gradients and hydration force. *Biochimica et Biophysica Acta (BBA) - Biomembranes, 1104*, 226–232.
9. Xie, J., Ji, Y., Xue, W., Ma, D., & Hu, Y. (2018). Hyaluronic acid-containing ethosomes as a potential carrier for transdermal drug delivery. *Colloids and Surfaces B: Biointerfaces, 172*, 323–329.

10. Indulekha, S., Arunkumar, P., Bahadur, D., & Srivastava, R. (2016). Thermoresponsive polymeric gel as an on-demand transdermal drug delivery system for pain management. *Materials Science and Engineering: C, 62*, 113–122.
11. Zhou, X., Hao, Y., Yuan, L., Pradhan, S., Shrestha, K., Pradhan, O., Liu, H., & Li, W. (2018). Nano-formulations for transdermal drug delivery: A review. *Chinese Chemical Letters, 29*, 1713–1724.
12. Mbah, C. C., Builders, P. F., & Attama, A. A. (2014). Nanovesicular carriers as alternative drug delivery systems: Ethosomes in focus. *Expert Opinion on Drug Delivery, 11*, 45–59.
13. Fang, J.-Y., Hwang, T.-L., Huang, Y.-L., & Fang, C.-L. (2006). Enhancement of the transdermal delivery of catechins by liposomes incorporating anionic surfactants and ethanol. *International Journal of Pharmaceutics, 310*, 131–138.
14. Zhu, X., Li, F., Peng, X., & Zeng, K. (2013). Formulation and evaluation of lidocaine base ethosomes for transdermal delivery. *Anesthesia and Analgesia, 117*, 352–357.
15. Bendas, E. R., & Tadros, M. I. (2007). Enhanced transdermal delivery of salbutamol sulfate via ethosomes. *AAPS PharmSciTech, 8*, E107–E107.
16. Shelke, S., Shahi, S., Jalalpure, S., & Dhamecha, D. (2016). Poloxamer 407-based intranasal thermoreversible gel of zolmitriptan-loaded nanoethosomes: formulation, optimization, evaluation and permeation studies. *Journal of Liposome Research, 26*, 1–11.
17. Iizhar, S. A., Syed, I. A., Satar, R., & Ansari, S. A. (2016). In vitro assessment of pharmaceutical potential of ethosomes entrapped with terbinafine hydrochloride. *Journal of Advance Research, 7*, 453–461.
18. Cui, Z., Zheng, Z., Lin, L., Si, J., Wang, Q., Peng, X., & Chen, W. (2018). Electrospinning and crosslinking of polyvinyl alcohol/chitosan composite nanofiber for transdermal drug delivery. *Advances in Polymer Technology, 37*, 1917–1928.
19. Gao, T., Jiang, M., Liu, X., You, G., Wang, W., Sun, Z., Ma, A., & Chen, J. (2019). Patterned polyvinyl alcohol hydrogel dressings with stem cells seeded for wound healing. *Polymers, 11*, 171.
20. Zhang, R., Zhang, X., Tang, Y., & Mao, J. (2020). Composition, isolation, purification and biological activities of Sargassum fusiforme polysaccharides: A review. *Carbohydrate Polymers, 228*, 115381.
21. Vandghanooni, S., & Eskandani, M. (2019). Electrically conductive biomaterials based on natural polysaccharides: Challenges and applications in tissue engineering. *International Journal of Biological Macromolecules, 141*, 636–662.
22. El-Fawal, G. (2014). Preparation, characterization and antibacterial activity of biodegradable films prepared from carrageenan. *Journal of Food Science and Technology, 51*, 2234–2239.
23. Sessarego, S., Rodrigues, S. C. G., Xiao, Y., Lu, Q., & Hill, J. M. (2019). Phosphonium-enhanced chitosan for Cr(VI) adsorption in wastewater treatment. *Carbohydrate Polymers, 211*, 249–256.
24. El-Haddad, M. N. (2014). Hydroxyethylcellulose used as an eco-friendly inhibitor for 1018 c-steel corrosion in 3.5% NaCl solution. *Carbohydrate Polymers, 112*, 595–602.
25. El Fawal, G. F., Abu-Serie, M. M., Hassan, M. A., & Elnouby, M. S. (2018). Hydroxyethyl cellulose hydrogel for wound dressing: Fabrication, characterization and in vitro evaluation. *International Journal of Biological Macromolecules, 111*, 649–659.
26. El Fawal, G., Hong, H., song, X., Wu, J., Sun, M., He, C., Mo, X., Jiang, Y., & Wang, H. (2020). Fabrication of antimicrobial films based on hydroxyethylcellulose and ZnO for food packaging application. *Food Packaging and Shelf Life, 23*, 100462.
27. Shew, R. L., & Deamer, D. W. (1985). A novel method for encapsulation of macromolecules in liposomes. *Biochimica et Biophysica Acta (BBA) - Biomembranes, 816*, 1–8.
28. Zhang, L., Wang, J., Chi, H., & Wang, S. (2016). Local anesthetic lidocaine delivery system: chitosan and hyaluronic acid-modified layer-by-layer lipid nanoparticles. *Drug Delivery, 23*, 3529–3537.
29. Nezarati, R. M., Eifert, M. B., & Cosgriff-Hernandez, E. (2013). Effects of humidity and solution viscosity on electrospun fiber morphology. *Tissue Engineering Methods (Part C), 19*, 810–819.
30. Athira, K. S., Sanpui, P., & Kaushik, C. (2014). Fabrication of poly(Caprolactone) nanofibers by electrospinning. *Journal of Polymer Science Part B: Polymer Physics, 2*, 62–66.
31. Chahal, S., Hussain, F. S. J., Kumar, A., Rasad, M. S. B. A., & Yusoff, M. M. (2016). Fabrication, characterization and in vitro biocompatibility of electrospun hydroxyethyl cellulose/poly (vinyl) alcohol nanofibrous composite biomaterial for bone tissue engineering. *Chemical Engineering Science, 144*, 17–29.
32. Krupa, A., Jaworek, A., Sobczyk, A.T., Lackowski, M., Czech, T., Ramakrishna, S., Sundarrajan, S.,& Pliszka D. (2008).Electrosprayed nanoparticles for nanofiber coating. ILASS 2008 Sep. 8-10, Como Lake, Italy (Paper ID ILASS08-P-13).
33. Touitou, E., Dayan, N., Bergelson, L., Godin, B., & Eliaz, M. (2000). Ethosomes-novel vesicular carriers for enhanced delivery: Characterization and skin penetration properties. *Journal of Control Release, 65*, 403–418.

34. Kostakova, E., Zemanová, E., Mikeš, P., Soukupova, J., Matheisová, H., & Klouda, K. (2012). Electrospinning and electrospraying of polymer solutions with spherical fullerenes. In *NANOCON 2012 - Conference Proceedings, 4th International Conference* (pp. 435–439).
35. Zulkifli, F. H., Hussain, F. S. J., Harun, W. S. W., & Yusoff, M. M. (2019). Highly porous of hydroxyethyl cellulose biocomposite scaffolds for tissue engineering. *International Journal of Biological Macromolecules, 122*, 562–571.
36. Andrade, G., Barbosa-Stancioli, E. F., Mansur, A. A. P., Vasconcelos, W. L., & Mansur, H. S. (2006). Design of novel hybrid organic-inorganic nanostructured biomaterials for immunoassay applications. *Biomedical Materials., 1*, 221.
37. Coates, J., (2000). Interpretation of infrared spectral, encyclopedia of analytical chemistry. John Wiley & Sons, Ltd, Chichester, p. 10815.
38. Kumar, A., Negi, Y. S., Bhardwaj, N. K., & Choudhary, V. (2012). Synthesis and characterization of methylcellulose/PVA based porous composite. *Carbohydrate Polymers, 88*, 1364–1372.
39. Li, J., Revol, J. F., & Marchessault, R. H. (1997). Effect of degree of deacetylation of chitin on the properties of chitin crystallites. *Journal of Applied Polymer Science, 65*, 373.
40. Qua, E. H., Hornsby, P. R., Sharma, H. S. S., Lyons, G., & McCall, R. D. (2009). Preparation and characterization of poly(vinyl alcohol) nanocomposites made from cellulose nanofibers. *Journal of Applied Polymer Science, 113*, 2238–2247.
41. Jiang, L., Li, X., Liu, L., & Zhang, Q. (2013). Cellular uptake mechanism and intracellular fate of hydrophobically modified pullulan nanoparticles. *International Journal of Nanomedicine, 8*, 1825–1834.
42. Kampmann, A.-L., Grabe, T., Jaworski, C., & Weberskirch, R. (2016). Synthesis of well-defined core–shell nanoparticles based on bifunctional poly(2-oxazoline) macromonomer surfactants and a microemulsion polymerization process. *RSC Advances, 6*, 99752–99763.
43. Dhiman, A., & Singh, D. (2013). Development, characterization & in vitro skin permeation of rutin ethosomes as a novel vesicular carrier. *International Journal of Biomedical Research, 4*, 559.
44. Asran, A. S., Henning, S., & Michler, G. H. (2010). Polyvinyl alcohol–collagen–hydroxyapatite biocomposite nanofibrous scaffold: Mimicking the key features of natural bone at the nanoscale level. *Polymer, 51*, 868–876.
45. Russo, R., Abbate, M., Malinconico, M., & Santagata, G. (2010). Effect of polyglycerol and the crosslinking on the physical properties of a blend alginate-hydroxyethyl cellulose. *Carbohydrate Polymers, 82*, 1061–1067.
46. Guirguis, O. W., & Moselhey, M. T. H. (2012). Thermal and structural studies of poly (vinyl alcohol) and hydroxypropyl cellulose blends. *Natural Science, 04*(01), 11.
47. Holland, B. J., & Hay, J. N. (2001). The thermal degradation of poly(vinyl alcohol). *Polymer, 42*, 6775–6783.
48. Ali, I. O. (2013). Synthesis and characterization of Ag0/PVA nanoparticles via photo- and chemical reduction methods for antibacterial study. *Colloids and Surfaces A: Physicochemical and Engineering Aspects, 436*, 922–929.
49. Attia, G., & Abd El-kader, M. (2013). Structural, optical and thermal characterization of PVA/2HEC polyblend films. *International Journal of Electrochemical Science, 8*, 5672–5687.
50. Chen, R., Yi, C., Wu, H., & Guo, S. (2010). Degradation kinetics and molecular structure development of hydroxyethyl cellulose under the solid state mechanochemical treatment. *Carbohydrate Polymers, 81*, 188–195.
51. Sakdiset, P., Amnuaikit, T., Pichayakorn, W., & Pinsuwan, S. (2019). Formulation development of ethosomes containing indomethacin for transdermal delivery. *Journal of Drug Delivery Science and Technology, 52*, 760–768.
52. Niu, X.-Q., Zhang, D.-P., Bian, Q., Feng, X.-F., Li, H., Rao, Y.-F., Shen, Y.-M., Geng, F.-N., Yuan, A.-R., Ying, X.-Y., & Gao, J.-Q. (2019). Mechanism investigation of ethosomes transdermal permeation. *International Journal of Pharmaceutics: X, 1*, 100027.